BIOCHEMISTRY
including biophysical chemistry & molecular biology

Article

pubs.acs.org/biochemistry

Resonance Raman Spectra of Five-Coordinate Heme-Nitrosyl Cytochromes *c′*: Effect of the Proximal Heme-NO Environment

Amy E. Servid,[†] Alison L. McKay,[†] Cherry A. Davis,[†] Elizabeth M. Garton,[†] Andreea Manole,[‡,§] Paul S. Dobbin,[‡] Michael A. Hough,[‡] and Colin R. Andrew*[,†]

[†]Department of Chemistry & Biochemistry, Eastern Oregon University, La Grande, Oregon 97850, United States
[‡]School of Biological Sciences, University of Essex, Wivenhoe Park, Colchester CO4 3SQ, U.K.

Supporting Information

ABSTRACT: Five-coordinate heme nitrosyl complexes (5cNO) underpin biological heme-NO signal transduction. Bacterial cytochromes *c′* are some of the few structurally characterized 5cNO proteins, exhibiting a distal to proximal 5cNO transition of relevance to NO sensing. Establishing how 5cNO coordination (distal vs proximal) depends on the heme environment is important for understanding this process. Recent 5cNO crystal structures of *Alcaligenes xylosoxidans* cytochrome *c′* (AXCP) and *Shewanella frigidimarina* cytochrome *c′* (SFCP) show a basic residue (Arg124 and Lys126, respectively) near the proximal NO binding sites. Using resonance Raman (RR) spectroscopy, we show that structurally characterized 5cNO complexes of AXCP variants and SFCP exhibit a range of ν(NO) (1651−1671 cm^{-1}) and ν(FeNO) (519−536 cm^{-1}) vibrational frequencies, depending on the nature of the proximal heme pocket and the sample temperature. While the AXCP Arg124 residue appears to have little impact on 5cNO vibrations, the ν(NO) and ν(FeNO) frequencies of the R124K variant are consistent with (electrostatically) enhanced Fe(II) → (NO)π* backbonding. Notably, RR frequencies for SFCP and R124A AXCP are significantly displaced from the backbonding trendline, which in light of recent crystallographic data and density functional theory modeling may reflect changes in the Fe−N−O angle and/or extent of σ-donation from the NO(π*) to the Fe(II) (d_{z^2}) orbital. For R124A AXCP, correlation of vibrational and crystallographic data is complicated by distal and proximal 5cNO populations. Overall, this study highlights the complex structure−vibrational relationships of 5cNO proteins that allow RR spectra to distinguish 5cNO coordination in certain electrostatic and steric environments.

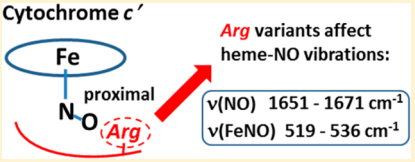

Complexes of nitric oxide (NO) with heme protein Fe-porphyrinate cofactors are important in cellular signaling, immune defense, and response to nitrosative stress.[1,2] Unique among diatomic gases, NO exhibits a negative trans effect in six-coordinate Fe(II)NO heme complexes (6cNO), promoting the release of the endogenous (His) protein ligand to form a five-coordinate heme-nitrosyl (5cNO) with NO as the sole axial ligand.[3,4] Although most heme-nitrosyl proteins remain in the 6cNO state because of the "cage effect" of the surrounding protein structure, 5cNO formation does occur in a subset of proteins, including soluble guanylate cyclase (sGC) and certain other heme nitric oxide/oxygen binding (H-NOX) gas sensors that selectively form 5cNO complexes (while excluding O_2).[5] Conformational changes associated with 5cNO formation are believed to underpin the NO sensing and signal transduction mechanisms of these proteins. Bacterial cytochromes *c′*, which protect against nitrosative stress, are some of the few heme proteins to have been structurally characterized in their 5cNO state.[6−8] Near-atomic resolution structures have recently been reported for 5cNO complexes of *Alcaligenes xylosoxidans* cytochrome *c′* [AXCP, Protein Data Bank (PDB) entry 2xlm][7] and *Shewanella frigidimarina* cytochrome *c′* (SFCP, PDB entry 4cx9),[8] as well as for several AXCP variants with mutations of proximal pocket residues (PDB entries 2xle, 2xlo, 2xlv, 2xlw, and 2xl6).[7] A surprising feature of these 5cNO complexes is the location of the NO ligand on the proximal (rather than distal) heme face in place of the His ligand. Time-resolved absorption measurements of binding of NO to AXCP suggest that the proximal 5cNO product is formed via a series of distal heme-NO intermediates, including 6cNO and putative distal 5cNO and dinitrosyl species.[7,9] This unexpected distal → proximal heme-NO conversion has expanded the repertoire of heme-NO reaction mechanisms in proteins,[7,9] with distal versus proximal 5cNO coordination emerging as a potential strategy for selective NO response. Indeed, very recently, a proximal 5cNO binding mode was confirmed in the crystal structure of H-NOX from *Shewanella oneidensis*.[10] Mechanistic studies also support distal → proximal 5cNO conversion in sGC,[11,12] the proapoptotic cytochrome *c*/cardiolipin complex,[13] cystathionine *β*-synthase,[14] and the dissimilative nitrate respiration (DNR) regulator.[15]

Resonance Raman (RR) spectroscopy is a powerful technique for probing the structures of heme-XO gas complexes (X = C, O, or N) via trends in ν(XO) and ν(FeXO) stretching frequencies, the values of which can be determined from their frequency shifts with isotopically labeled

Received: March 3, 2015
Revised: April 22, 2015
Published: May 11, 2015

DOI: 10.1021/acs.biochem.5b00227
Biochemistry 2015, 54, 3320−3327

gases.[16,17] RR spectra of 5cNO complexes are characterized by ν(NO) vibrations in the range of 1650−1700 cm^{-1}, with isotope downshifts of ∼30 cm^{-1} (^{15}NO) or ∼65 cm^{-1} ($^{15}N^{18}O$).[18] Although the inherently bent Fe−N−O geometry allows mixing to occur between the ν(FeNO) stretching and δ(FeNO) bending modes, 5cNO RR spectra exhibit only one (N)O isotope-sensitive RR band in the 510−540 cm^{-1} region attributed to a predominant ν(FeNO) stretch, with downshifts of ∼10 cm^{-1} (^{15}NO) or ∼15 cm^{-1} ($^{15}N^{18}O$).[18] Results of nuclear resonance vibrational spectroscopy (NRVS) studies of 5cNO porphyrins concur with this ν(FeNO) assignment,[19−21] while also establishing the predominant δ(FeNO) bending mode (not observed in RR spectra) at a lower frequency (∼380−400 cm^{-1}).[19,21] An important determinant of heme-XO vibrations is the extent of Fe(II) → XO(π^*) backbonding that strengthens the Fe-XO interaction while weakening the X-O bond, leading to a negative correlation between ν(FeXO) and ν(XO) frequencies.[17] Utilizing inductive effects to modulate backbonding (via porphyrin ring substitutions), RR studies have demonstrated negative correlations of ν(FeXO) versus ν(XO) for all three gas ligands, including 5cNO complexes.[17] Within protein molecules, heme-XO vibrations are also sensitive to the heme pocket environment, making RR spectroscopy a useful structural probe of the gas binding site. For example, extensive studies of heme-CO proteins have shown that positive charges and H-bond donors enhance backbonding (by stabilizing the buildup of negative charge on the CO ligand), whereas regions of electron density have the opposite effect.[16,17,22] For cytochromes c', ν(FeCO)/ν(CO) frequencies lie midway along the backbonding line, consistent with the nonpolar character (hydrophobic cage) of the distal pocket.[23,24]

By contrast, the effect of protein environments on 5cNO vibrations is much less defined. Aside from AXCP and SFCP, the only other crystal structures of 5cNO proteins published to date are for *S. oneidensis* H-NOX (proximal Fe−N−O angle of 126°)[10] and T-state nitrosyl hemoglobin α-subunits (distal Fe−N−O angles of 138°),[25] neither of which has corresponding RR data. Relative to those of heme-CO complexes, the inherently bent Fe−N−O geometries of Fe(II) nitrosyls (∼142° in unhindered 5cNO porphyrins) impart additional structural determinants on heme-XO vibrations.[26,27] Along with the expected enhancement of Fe(II) → NO(π^*) backbonding by positive charges,[28] DFT modeling predicts an intricate dependence of ν(NO) and ν(FeNO) frequencies on the Fe−N−O bond angle.[27] Although hydrogen bonding to the NO ligand appears to be relatively weak,[29,30] DFT calculations for 6cNO complexes predict an inverse correlation of ν(FeNO) and ν(NO) frequencies for H-bonding to the NO oxygen atom or the N−O bond, whereas H-bonding to the nitrogen of NO should lead to a decrease in both ν(FeNO) and ν(NO).[26] Studies of axial ligation in Fe(II)NO porphyrins also point to a direct correlation of ν(FeNO) and ν(NO) frequencies arising from changes in σ donation from the NO(π^*) orbital to the Fe(II)(d_{z^2}) orbital.[2] Inductive effects may also modulate the ν(FeNO) and ν(NO) frequencies of some 5cNO proteins, given that recent studies attribute weak backbonding in the sGC CO complex to the electron withdrawing properties of strongly H-bonded heme propionates.[31]

Crystal structures of 5cNO cytochromes c' reveal significant differences between the distal and proximal heme environments. Whereas the distal heme face is crowded with hydrophobic residues, a conserved basic residue (Arg124 in AXCP and Lys126 in SFCP) is positioned near the endogenous His and proximal NO binding sites.[7,8,32] Although this basic residue is not an absolute requirement for proximal 5cNO coordination, kinetic studies of AXCP show that Arg124 hinders His-Fe bond scission prior to proximal NO binding[7] and also impedes the release of NO from the proximal pocket.[33] Reasoning that the distinct heme pocket polarities of cytochromes c' should lead to backbonding differences between distal and proximal NO ligands, we previously attributed the relatively low ν(NO) frequency of native 5cNO AXCP (1661 cm^{-1} at room temperature) to proximal NO coordination with enhanced backbonding due to the positive charge of the nearby Arg124.[23] However, the influence of protein environments on 5cNO vibrations has yet to be systematically studied. Here we report 5cNO RR measurements on structurally characterized AXCP variants in which Arg124 (adjacent to the proximal NO site) is replaced with residues of different sizes and polarities (Lys, Phe, Gln, Glu, and Ala).[7] We also obtained 5cNO RR data for SFCP that has a native Lys residue instead of Arg (adjacent to the proximal NO ligand) and a relatively small Fe−N−O angle of ∼128°.[8] Trends in ν(NO) and ν(FeNO) frequencies for the 5cNO cytochromes are discussed with respect to their X-ray crystal structures, together with predictions from recent RR and DFT studies.

EXPERIMENTAL PROCEDURES

Materials. Purified protein samples of AXCP and SFCP were prepared as previously described.[8,34] Protein solutions for RR measurements (∼300−700 μM in heme) were typically prepared in pH 7.0 buffer (50 mM MOPS and 0.10 M NaCl) inside an anaerobic glovebox. Additional samples were prepared in buffers containing 0.10 M NaCl and either 50 mM CHES (pH 9.5) or 50 mM sodium acetate (pH 5.0). Ferric protein solutions were reduced to the ferrous state using a 20-fold excess of sodium dithionite, followed by removal of excess dithionite with a minispin desalting column (Zeba filter, Pierce). Ferrous proteins were transferred to septum-sealed anaerobic capillary tubes and reacted with 0.6 mL of either ^{14}NO or isotope-labeled (^{15}NO or $^{15}N^{18}O$) gas (Cambridge Isotope Laboratories) that had been bubbled through a 0.1 M KOH solution to remove higher oxides of nitrogen. After equilibration for 5 min, the presence of 5cNO coordination in each RR capillary was confirmed by optical absorption using a modified Cary 50 UV−visible spectrophotometer.

Spectroscopy. Resonance Raman (RR) spectra were recorded on a custom McPherson 2061/207 spectrograph (set to a 0.67 m focal length with a 100 μm slit width and a 2400 grooves/mm holographic grating) equipped with a Princeton Instruments liquid N_2-cooled (LN1100PB) CCD detector. Excitation wavelengths of 406.7 and 413.1 nm were provided by a krypton ion laser, and the Rayleigh line was attenuated using a supernotch filter (Kaiser) or a long-pass filter (RazorEdge, Semrock). To help maintain sample integrity, and to match the temperature of crystals used in previous structural studies,[7] the majority of RR measurements were performed on frozen solutions maintained at 100 K by means a liquid nitrogen-cooled coldfinger. RR spectra at 100 K were recorded using laser powers of 4−70 mW (at the sample) and an ∼150° backscattering geometry. Additional room-temperature RR spectra were recorded in a 90° scattering geometry using lower laser powers (0.5−2 mW at the sample) and a reciprocating translation stage. Protein RR spectra were

DOI: 10.1021/acs.biochem.5b00227
Biochemistry 2015, 54, 3320−3327

typically measured over a period of 2−5 min, using an aspirin standard to calibrate Raman shifts to an accuracy of ±1 cm^{-1}.

RESULTS AND DISCUSSION

5cNO RR Spectra. RR measurements on AXCP proteins were performed exclusively on frozen solutions (100 K). The effects of Arg124 mutations on 5cNO AXCP RR spectra are shown in the high-frequency (1330−1700 cm^{-1}) (Figure 1) and low-frequency (370−700 cm^{-1}) (Figure 2) regions. Porphyrin marker bands of wild-type (wt) AXCP [ν_4 (1375 cm^{-1}), ν_3 (1510 cm^{-1}), ν_2 (1595 cm^{-1}), and ν_{10} (1645 cm^{-1}) (Figure 1A)] are typical of 5c low-spin heme and resemble frequencies previously reported for native 5cNO AXCP at 90 K[23] (Table 1). Isotopic replacement with ^{15}NO identifies the wt AXCP ν(NO) vibration at 1664 cm^{-1} from its frequency shift of −31 cm^{-1} with ^{15}NO (Figure 1A) and −65 cm^{-1} with $^{15}N^{18}O$ (Figure S1 of the Supporting Information). Among the R124 variant 5cNO complexes, porphyrin marker bands occur at frequencies (±3 cm^{-1}) similar to those of wt AXCP (Figure 1B−F and Table 1). While the ν(NO) frequencies of R124F, R124Q, and R124E variants are within 3 cm^{-1} of that of wt AXCP, larger variations are observed for R124K (1657 cm^{-1}) and R124A (1671 cm^{-1}) (Figure 1B−F and Table 1). In the low-frequency RR region (Figure 2), the ν(FeNO) frequency of wt 5cNO AXCP is identified at 531 cm^{-1} (Figure 2A) from its 16 cm^{-1} downshift with $^{15}N^{18}O$ (Figure 2A), and by its 11 cm^{-1} downshift with ^{15}NO (data not shown). Among the AXCP variants, ν(FeNO) frequencies range from 529 cm^{-1} (R124F) to 536 cm^{-1} (R124A) (Figure 2 and Table 1).

In the case of SFCP (Lys126 adjacent to the proximal NO site), RR spectra were recorded at both 100 K and room temperature (Figures 3 and 4), the latter requiring very low laser powers (~0.5−2 mW) and an oscillating sample. At 100 K, 5cNO SFCP porphyrin marker bands [ν_4 (1375 cm^{-1}), ν_3

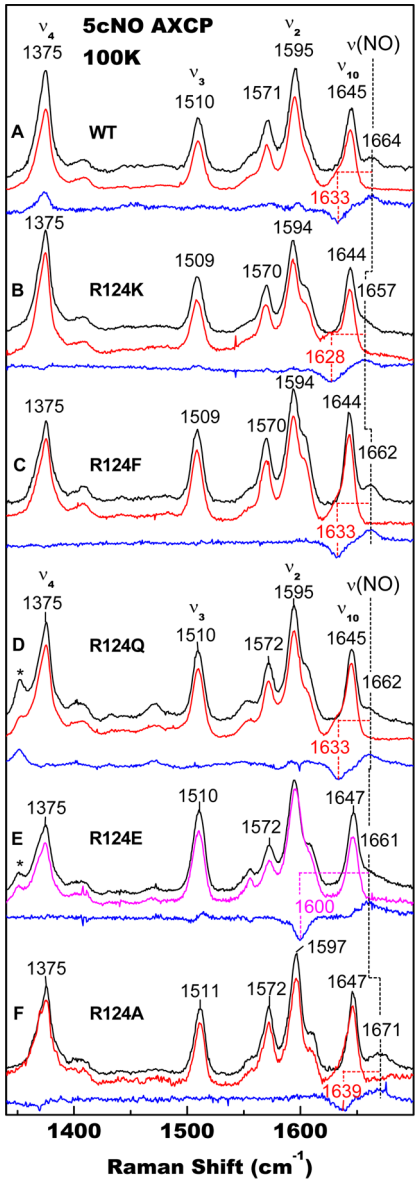

Figure 1. High-frequency RR spectra of 5cNO AXCP at 100 K: (A) wt, (B) R124K, (C) R124F, (D) R124Q, (E) R124E, and (F) R124A proteins prepared with ^{14}NO (black), ^{15}NO (red), and $^{15}N^{18}O$ (magenta). Isotope difference spectra (blue) reveal the presence of ν(NO) vibrations.

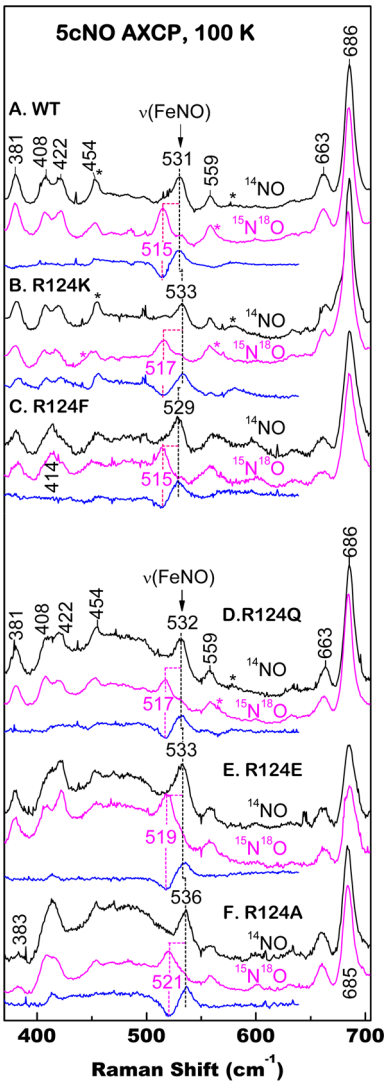

Figure 2. Low-frequency RR spectra of 5cNO AXCP at 100 K: (A) wt, (B) R124K, (C) R124F, (D) R124Q, (E) R124E, and (F) R124A proteins prepared with ^{14}NO (black) and $^{15}N^{18}O$ (magenta). Isotope difference spectra (^{14}NO − $^{15}N^{18}O$, blue) reveal the presence of ν(FeNO) vibrations. Asterisks denote vibrations attributed to a minor 6cNO population.

DOI: 10.1021/acs.biochem.5b00227
Biochemistry 2015, 54, 3320−3327

Table 1. RR Frequencies (cm^{-1}) of 5cNO Proteins

protein	temp	ν_4	ν_3	ν_2	ν_{10}	ν(NO)	ν(FeNO)	ref
				5cNO Cytochromes c'[a]				
AXCP, wt (R124)	100 K	1375	1510	1595	1645	1664	531	this work
	rt	1373	1506	1592	1641	1661	526	23
	100 K	(1378)	(1512)	(1597)	(1648)	nd	nd	35
R124K	100 K	1375	1509	1594	1644	1657	533	this work
R124F	100 K	1375	1509	1594	1644	1662	529	this work
R124Q	100 K	1375	1510	1595	1645	1662	532	this work
R124E	100 K	1375	1510	1595	1647	1661	533	this work
R124A	100 K	1375	1511	1597	1647	1671	536	this work
SFCP, wt (K126)	100 K	1375	1508	1591	1643	1651	525	this work
	rt	1373	1505	1589	1640	1658	519	this work
RCCP, K42E (R126)	rt	1367	1511	1594	1648	1666	523	40
				Other 5cNO Proteins				
horse myoglobin, pH 4	rt					1668	524	41
sperm whale H93G	nr					1670	535	42
H93Y	nr	nr	nr	nr	nr	1672	524	43
$Fe_BMb1(NO)_2$	110 K	1375	1506	1586	1644	1660	522	44
CooA	nr	1376	1506	1582	1641	1672	523	45
sGC (excess NO)	rt	1375	1509	1585	1645	1680	522	27
sGC, YC-1, and GTP	rt					1700	521	46
FixL	rt	nr	1509	nr	1646	1675	525	47

[a]Cytochrome c' RR frequencies are for protein solutions at pH 7.0, except for data in parentheses obtained from single crystals at pH 7.5. Abbreviations: rt, room temperature; nr, not reported; nd, not determined; AXCP, *A. xylosoxidans* cytochrome c'; SFCP, *S. frigidimarina* cytochrome c'; RCCP, *Rhodobacter capsulatus* cytochrome c'; $Fe_BMb1(NO)_2$, 5cNO product of the L29H/F43H/V68E triple variant of Mb.

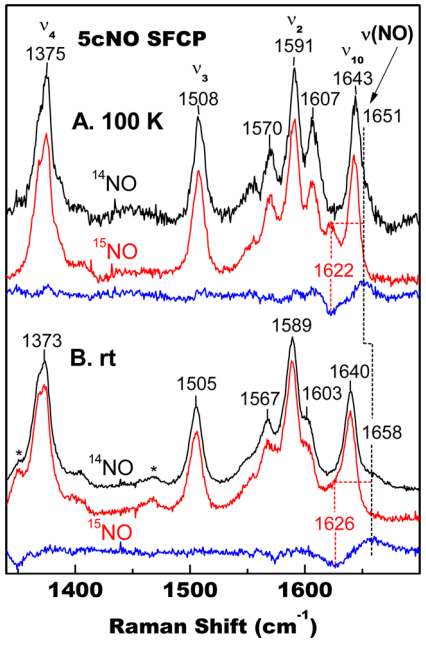

Figure 3. High-frequency RR spectra of 5cNO wt SFCP at (A) 100 K and (B) room temperature prepared with ^{14}NO (black) and ^{15}NO (red). Isotope difference spectra (^{14}NO − ^{15}NO, blue) reveal the presence of ν(NO) vibrations.

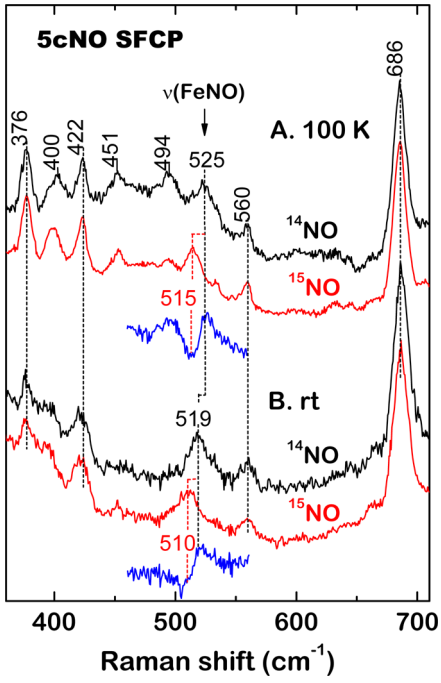

Figure 4. Low-frequency RR spectra of 5cNO wt SFCP at (A) 100 K and (B) room temperature prepared with ^{14}NO (black) and ^{15}NO (red). Isotope difference spectra (^{14}NO − ^{15}NO, blue) reveal the presence of ν(FeNO) vibrations.

(1508 cm^{-1}), ν_2 (1591 cm^{-1}), and ν_{10} (1643 cm^{-1}) (Figure 3A)] are within 1−4 cm^{-1} of those observed for AXCP (Table 1). Isotopic substitution with ^{15}NO identifies ν(NO) at 1651 cm^{-1} (Figure 3A) and ν(FeNO) at 525 cm^{-1} (Figure 4A). Notably, the ν(NO) frequency of SFCP (1651 cm^{-1}) is lower than those for all of the AXCP complexes measured, with that of R124K AXCP being the closest (1657 cm^{-1}). Relative to the 100 K data, room-temperature SFCP 5cNO RR spectra show minor downshifts (2−3 cm^{-1}) in porphyrin marker frequencies (Figure 3B), as well as a 7 cm^{-1} increase in ν(NO) (1658 cm^{-1}) and a 6 cm^{-1} decrease in ν(FeNO) (519 cm^{-1}).

Influence of Heme-NO Environment on RR Frequencies. Figure 5 shows the relationship of RR frequencies for 5cNO proteins (Table 1) to the empirical ν(FeNO) versus ν(NO) backbonding line of model 5cNO porphyrins. Most of

DOI: 10.1021/acs.biochem.5b00227
Biochemistry 2015, 54, 3320−3327

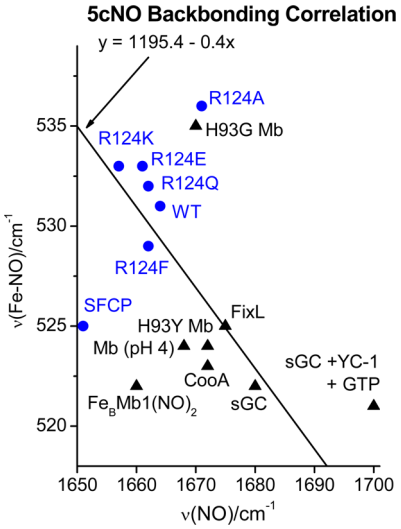

Figure 5. Correlation of ν(FeNO) and ν(NO) RR frequencies for 5cNO cytochromes c' at 100 K (circles) together with data from other 5cNO heme proteins at various temperatures (Table 1) (triangles). Superimposed is a plot of the experimental backbonding line previously determined in 5cNO model complexes.[17,18]

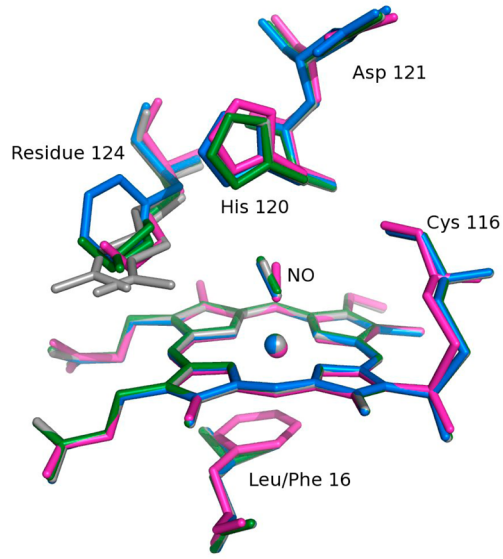

Figure 6. Superposition of heme pocket structures for the 5cNO complexes of native AXCP (gray), R124K (green), and R124F (blue) AXCP with monomer A of SFCP (magenta). AXCP structures were superposed using secondary structure matching in Coot, while SFCP was superposed onto the structure of the native AXCP 5cNO complex using all heme atoms. Note that residue numbering refers to the sequence of AXCP.

the cytochrome c' RR frequencies lie close to the backbonding line, with the notable exceptions of SFCP and R124A AXCP. The influence of the heme-NO environment on the vibrations of 5cNO cytochromes c' is discussed in light of their crystal structures,[7,8] as well as predictions from previous RR studies and DFT calculations.[2,17] X-ray crystal structures of the 5cNO complexes of AXCP and SFCP proteins reveal several key features.[7,8] With the exception of R124A AXCP (which forms a mixture of distal and proximal 5cNO species) all 5cNO structures show NO bound exclusively on the proximal heme face with no ligand bound to the distal face. A single location for the NO ligand is observed in the structures of wt, R124K, and R124F AXCP, together with wt SFCP (Figure 6), while the other AXCP variants (R124Q, R124E, and R124A) exhibit multiple FeNO conformers. Variations in the Fe−N−O angle (128−146°) are observed among the different 5cNO crystal structures. The R124Q and R124E variants contain polar residues adjacent to the NO ligand, and these may form a hydrogen bond to one of the observed NO conformers. The remaining variants and native AXCP do not utilize H-bonding to stabilize the NO ligand (the apparent H-bond reported in an earlier crystal structure of 5cNO native AXCP[6] was not present in a subsequent higher-resolution structure[7]).

We first consider 5cNO RR frequency trends for cytochromes c' with single crystallographic heme-NO conformations: AXCP (wt, R124F, and R124K) and SFCP. It has been proposed that positive electrostatic environments strengthen backbonding in ferrous-nitrosyl proteins, yielding higher ν(FeNO) frequencies and lower ν(NO) frequencies.[28] Consistent with this idea, the R124K variant of AXCP (positive proximal residue) has a lower ν(NO) frequency and a higher ν(FeNO) frequency compared to those of R124F (neutral residue) (Table 1 and Figure 5). On the other hand (and contrary to previous suggestions), the basic Arg124 residue in native AXCP appears to have little influence on backbonding because its ν(NO) and ν(FeNO) frequencies are similar to those of the nonpolar variant, R124F (Table 1 and Figure 5). While the N(O)−Arg distance in wt AXCP (4.0 Å) is shorter than the N(O)−Lys distance in R124K AXCP (5.2 Å), charge delocalization within the Arg guanidino group may decrease the electrostatic field relative to the Lys ε-amino group. In comparison, the N(O)−Lys Nζ distance in SFCP is some 5.9 Å. For SFCP, it is notable that the 5cNO RR frequencies lie significantly below the backbonding line (Figure 5), with ν(NO) and ν(FeNO) frequencies being lower than those of any of the 5cNO AXCP complexes (Table 1). Recent DFT modeling of 5cNO porphyrins predicts that compressing the Fe−N−O angle below the equilibrium value of 142° should decrease both the ν(NO) and ν(FeNO) frequencies, whereas modest increases in the Fe−N−O angle (to 142−150°) are predicted to boost the ν(NO) frequency with smaller increases in ν(FeNO).[27] In light of these DFT predictions, the lower ν(NO) and ν(FeNO) frequencies of SFCP (Table 1) may be due to the former having a relatively compressed Fe−N−O angle (128° in the SFCP crystal structure). Electrostatic enhancement of heme-NO backbonding (due to the positive Lys126 side chain) might also act synergistically with Fe−N−O angle compression to further lower the SFCP ν(NO) value, while offsetting the angle-induced decrease in ν(FeNO). It is also noted that a direct correlation of ν(FeNO) and ν(NO) frequencies in Fe(II)NO complexes is a hallmark of a change in NO(π^*) → $Fe^{2+}(d_{z^2})$ σ bonding.[2]

Three of the AXCP variants (R124Q, -E, and -A) exhibit multiple heme-NO conformers in their 5cNO crystal structures. For R124Q, two positions of the proximal Fe−NO unit are apparent: one pointed toward $O^{\varepsilon 1}$ of Gln124 (at 2.9 Å) and the other toward the main chain carbonyl (O) of Cys116 (3.3 Å).[7] Two proximal Fe−NO orientations are also evident in the R124E crystal structure: one oriented toward the carbonyl (O) of Cys116 (at 3.0 Å) and the other apparently H-bonded to $O^{\varepsilon 1}$ of Glu124 (at 2.9 Å).[7] However, because the ν(FeNO) and ν(NO) RR frequencies of R124Q (~1662 cm^{-1}) and R124E (~1661 cm^{-1}) variants are similar to those of wt and R124F

DOI: 10.1021/acs.biochem.5b00227
Biochemistry 2015, 54, 3320−3327

AXCP (Figure 1 and Table 1), it appears that the Gln and Glu residues have little influence on 5cNO backbonding.

Notably, R124A AXCP exhibits both the highest ν(NO) (1671 cm^{-1}) and highest ν(FeNO) (536 cm^{-1}) values of all the 5cNO cytochromes c' (Figures 1F and 2F and Table 1), with frequencies located significantly above the backbonding line (Figure 5). According to previous DFT model calculations, an increase in both the ν(FeNO) and ν(NO) frequency might arise from a relatively large Fe−N−O angle[27] and/or an increase in NO(π^*) → $Fe^{2+}(d_{z^2})$ σ bonding.[2] Uniquely among the 5cNO crystal structures, that of R124A AXCP exhibits a mixture of proximal and distal 5cNO binding modes, a feature attributed to the conformation of the displaced His ligand (which may partially block bimolecular binding of NO to the proximal site) as well as to displacement of the heme group toward the proximal pocket (creating a more favorable steric environment for distal heme-NO coordination).[7] In the distal 5cNO population (occupancy of 0.3), the NO ligand interacts solely with the nonpolar Leu16 residue and has a relatively large Fe−N−O angle of 146°. By contrast, the proximal 5cNO population (occupancy of 0.7) (existing in two conformations) has Fe−N−O angles of 126° and 140° and a hydrogen bond to the His ligand. However, given the multiple heme-NO conformers evident in R124A and other AXCP variant structures, establishing the connection between crystallographic Fe−N−O angles and observed RR frequencies is not straightforward.

Despite the heterogeneity evident within the 5cNO crystal structures of R124Q, -E, and -A variants, it is notable that their ν(FeNO) and ν(NO) RR bandwidths (in solution) resemble those of the other AXCP variants and SFCP (Figures 1−4) whose crystal structures show single heme-NO conformations.[7] The singlet nature of the RR bands of R124Q, -E, and -A variants suggests two possible scenarios: (i) different heme-NO conformers within each protein give rise to similar RR frequencies (such that multiple features are not resolved), or (ii) only one detectable heme-NO conformer is present in each RR (solution) sample. Although this RR study cannot distinguish between these two scenarios, it is striking that the R124A ν(NO) frequency determined from RR spectra (~1671 cm^{-1}) (Figure 1 and Table 1) is quite different from that of the predominant FTIR ν(NO) band (~1655 cm^{-1}) observed in recent geminate recombination studies.[39] The source of this discrepancy is puzzling, although it may be connected to the different sample conditions, e.g., FTIR (25 °C, pD 9.4) versus RR (100 K, pH 7.0). Although pH variations (5.0−9.5) have relatively little impact on R124A RR spectra (Figures S1 and S2 and Table S1 of the Supporting Information), the influence of temperature and protein/NO concentration on 5cNO R124A vibrations is not known. A tantalizing possibility is that the different sample conditions of RR and FTIR measurements favor alternate 5cNO R124A populations (predominantly distal or predominantly proximal), in which case structural differences between these populations (e.g., Fe−N−O angle) might conceivably account for the discrepancy between RR and FTIR ν(NO) values, as well as for the deviation of the R124A vibrations from the backbonding line.

Temperature Dependence of RR Frequencies. While the majority of 5cNO RR measurements in this study were performed at 100 K to ensure sample integrity (and to match the temperature of crystal structures), additional room-temperature RR data for wt AXCP and SFCP show that sample temperature can cause significant changes in 5cNO RR frequencies (Table 1). Relative to room temperature, the small downshifts (2−3 cm^{-1}) in porphyrin marker bands upon cooling to 100 K (Table 1) are a general feature of heme complexes attributed to contraction of the porphyrin core.[24,36,37] Of more interest are the temperature dependencies of the ν(FeNO) and ν(NO) frequencies. Relative to the 100 K data, the ν(FeNO) modes of AXCP and SFCP both decrease by 5−6 cm^{-1} at room temperature (Table 1). On the other hand, SFCP exhibits a 7 cm^{-1} increase in ν(NO) upon being warmed to room temperature, whereas AXCP shows a 2 cm^{-1} decrease (Table 1). The unique temperature dependencies of ν(NO) and ν(FeNO) may stem from changes in heme-NO conformation. Consistent with the conformational freedom of the heme-NO unit, warming the 5cNO SFCP sample from 100 K to room temperature also increases the half-height width of the ν(NO) RR vibrational envelope (from ~16 to ~25 cm^{-1}) (Figure 3). The presence of multiple heme-NO conformers at room temperature is supported by time-resolved FTIR absorption measurements of 5cNO formation in wt and R124A AXCP that show multiple ν(NO) components for both proteins, including a predominant ν(NO) band at ~1655 cm^{-1} with lower-intensity features at ~1665 and ~1675 cm^{-1}.[38,39] As well as the impact of sample temperature on 5cNO vibrations, it is also noted that vibrational frequencies in solution may differ from those in the crystalline state, even at similar temperatures. For example, single-crystal 5cNO RR data for wt AXCP[35] reveal porphyrin marker bands that are 2−3 cm^{-1} higher than those observed in solution at the same temperature (100 K) (Table 1), although the effect on the ν(FeNO) and ν(NO) frequencies is not known.

In summary, this study of 5cNO cytochromes c' represents the first analysis of RR frequency trends for structurally characterized 5cNO proteins. Overall, AXCP variant and wt SFCP proteins exhibit a 20 cm^{-1} span of ν(NO) frequencies (1651−1671 cm^{-1}) and a 17 cm^{-1} span of ν(FeNO) values (519−536 cm^{-1}), depending on the identity of residues in the proximal binding pocket and the sample temperature. Surprisingly, the native Arg124 residue of AXCP (nearest the proximal NO ligand) appears to have little impact on heme-NO bonding, because several variants (including R124F) exhibit ν(NO) and ν(FeNO) frequencies close to those of wt. On the other hand, the R124K mutation causes a 6 cm^{-1} decrease in ν(NO) and a 2 cm^{-1} increase in ν(FeNO) frequency, suggesting that a Lys side chain is more able to (electrostatically) enhance Fe(II) → NO(π^*) backbonding. The largest variations in ν(NO) and ν(FeNO) frequencies occur for SFCP and R124A AXCP, in both cases with significant deviations from the empirical backbonding line of model 5cNO porphyrins. In the case of SFCP, these deviations might arise from its relatively small Fe−N−O angle (128°)[7,27] and/or changes in NO(π^*) → $Fe^{2+}(d_{z^2})$ σ-bonding.[2] Interpretation of R124A AXCP vibrational data is complicated by the existence of distal and proximal 5cNO populations in its crystal structure. The singlet nature of its ν(NO) and ν(FeNO) RR bands suggests that these populations give rise to similar heme-NO frequencies or that only one detectable 5cNO population (proximal or distal) is present in solution. Further investigations of heme-NO vibrational determinants will be conducted as additional high-resolution structures of proximal and distal 5cNO proteins become available.

DOI: 10.1021/acs.biochem.5b00227
Biochemistry 2015, 54, 3320−3327

■ ASSOCIATED CONTENT

Supporting Information

Additional RR spectroscopic data (Table S1 and Figures S1 and S2). The Supporting Information is available free of charge on the ACS Publications website at DOI: 10.1021/acs.biochem.5b00227.

■ AUTHOR INFORMATION

Corresponding Author

*E-mail: candrew@eou.edu. Telephone: (541) 962-3322.

Present Address

§A.M.: Institute of Neurology, Queen Square, London WC1N 3BG, U.K.

Funding

This work was supported by National Science Foundation Grants MCB-0417152, MCB-0745035, and MCB-1411963 (to C.R.A.) and Royal Society Research Project Grant 120094 to M.A.H.

Notes

The authors declare no competing financial interest.

■ ACKNOWLEDGMENTS

We thank Dr. Pierre Moënne-Loccoz for assistance with RR measurements and Dr. Svetlana Antonyuk, Prof. Robert Eady, and Prof. Samar Hasnain for providing AXCP samples. Additional assistance was provided by David Pixton.

■ ABBREVIATIONS

5cNO, five-coordinate heme nitrosyl; 6cNO, six-coordinate heme nitrosyl; AXCP, cytochrome *c′* from *A. xylosoxidans*; DFT, density functional theory; H-NOX, heme nitric oxide/oxygen binding; RR, resonance Raman; sGC, soluble guanylate cyclase; SFCP, cytochrome *c′* from *S. frigidimarina*.

■ REFERENCES

(1) Ignarro, L. (2000) *Nitric Oxide: Biology and Pathobiology*, Academic Press, San Diego.

(2) Lehnert, N., Scheidt, W. R., and Wolf, M. W. (2014) Stucture and bonding in heme-nitrosyl complexes and implications for biology. *Struct. Bonding (Berlin, Ger.) 154*, 155−224.

(3) Scheidt, W. R., and Ellison, M. K. (1999) The synthetic and structural chemistry of heme derivatives with nitric oxide ligands. *Acc. Chem. Res. 32*, 350−359.

(4) Goodrich, L. E., Paulat, F., Praneeth, V. K., and Lehnert, N. (2010) Electronic structure of heme-nitrosyls and its significance for nitric oxide reactivity, sensing, transport, and toxicity in biological systems. *Inorg. Chem. 49*, 6293−6316.

(5) Tsai, A. L., Martin, E., Berka, V., and Olson, J. S. (2012) How Do Heme-Protein Sensors Exclude Oxygen? Lessons Learned from Cytochrome *c′*, *Nostoc puntiforme* Heme Nitric Oxide/Oxygen-Binding Domain, and Soluble Guanylyl Cyclase. *Antioxid. Redox Signaling 17*, 1246−1263.

(6) Lawson, D. M., Stevenson, C. E. M., Andrew, C. R., and Eady, R. R. (2000) Unprecedented proximal binding of nitric oxide to heme: Implications for guanylate cyclase. *EMBO J. 19*, 5661−5671.

(7) Hough, M. A., Antonyuk, S. V., Barbieri, S., Rustage, N., McKay, A. L., Servid, A. E., Eady, R. R., Andrew, C. R., and Hasnain, S. S. (2011) Distal to proximal NO conversion in hemoproteins: The role of the proximal pocket. *J. Mol. Biol. 405*, 395−409.

(8) Manole, A., Kekilli, D., Svistunenko, D. A., Wilson, M. T., Dobbin, P. S., and Hough, M. A. (2015) Conformational Control of the Binding of Diatomic Gases to cytochrome *c′*. *J. Biol. Inorg. Chem.*, DOI: 10.1007/s00775-015-1253-7.

(9) Pixton, D. A., Petersen, C. A., Franke, A., van Eldik, R., Garton, E. M., and Andrew, C. R. (2009) Activation parameters for heme-NO binding in *Alcaligenes xylosoxidans* cytochrome *c′*: The putative dinitrosyl intermediate forms via a dissociative mechanism. *J. Am. Chem. Soc. 131*, 4846−4853.

(10) Herzik, M. A. J., Jonnalagadda, R., Kuriyan, J., and Marletta, M. A. (2014) Structural insights into the role of iron-histidine bond cleavage in nitric oxide-induced activation of H-NOX gas sensor proteins. *Proc. Natl. Acad. Sci. U.S.A. 111*, E4156−E4164.

(11) Tsai, A.-L., Berka, V., Martin, F., Ma, X., van den Akker, F., Fabian, M., and Olson, J. S. (2010) Is *Nostoc* H-NOX a NO sensor or redox switch? *Biochemistry 49*, 6587−6599.

(12) Martin, E., Berka, V., Sharina, I., and Tsai, A. L. (2012) Mechanism of binding of NO to soluble guanylyl cyclase: Implication for the second NO binding to the heme proximal site. *Biochemistry 51*, 2737−2746.

(13) Silkstone, G., Kapetanaki, S. M., Husu, I., Vos, M. H., and Wilson, M. T. (2010) Nitric oxide binds to the proximal heme coordination site of the ferrocytochrome *c*/cardiolipin complex: Formation mechanism and dynamics. *J. Biol. Chem. 285*, 19785−19792.

(14) Vicente, J. B., Colaço, H. G., Mendes, M. I., Sarti, P., Leandro, P., and Giuffrè, A. (2014) NO* binds human cystathionine *β*-synthase quickly and tightly. *J. Biol. Chem. 289*, 8579−8587.

(15) Cutruzzolà, F., Arcovito, A., Giardina, G., dell Longa, S., D'Angelo, P., and Rinaldo, S. (2014) Distal−proximal crosstalk in the heme binding pocket of the NO sensor DNR. *BioMetals 27*, 763−773.

(16) Spiro, T. G., Ibrahim, M., and Wasbotten, I. H. (2008) in *The smallest biomolecules* (Ghosh, A., Ed.) pp 95−123, Elsevier, Amsterdam.

(17) Spiro, T. G., Soldatova, A. V., and Balakrishnan, G. (2013) CO, NO and O_2 as vibrational probes of heme protein interactions. *Coord. Chem. Rev. 257*, 511−527.

(18) Vogel, K. M., Kozlowski, P. M., Zgierski, M. Z., and Spiro, T. G. (1999) Determinants of the FeXO (X = C, N, O) vibrational frequencies in heme adducts from experiment and density functional theory. *J. Am. Chem. Soc. 121*, 9915−9921.

(19) Lehnert, N., Galinato, M. G. I., Paulat, F., Richter-Adido, G. B., Sturhahn, W., Xu, N., and Zhao, J. (2010) Nuclear resonance vibrational spectroscopy applied to [Fe(OEP)(NO)]: The vibrational assignments of five-coordinate ferrous heme-nitrosyls and implications for electronic structure. *Inorg. Chem. 49*, 4133−4148.

(20) Scheidt, W. R., Barabanschikov, A., Pavlik, J. W., Silvernail, N. J., and Sage, J. T. (2010) Electronic structure and dynamics of nitrosyl porphyrins. *Inorg. Chem. 49*, 6240−6252.

(21) Pavlik, J. W., Peng, Q., Silvernail, N. J., Alp, E. E., Hu, M. Y., Zhao, J., Sage, J. T., and Scheidt, W. R. (2014) Anisotropic iron motion in nitrosyl iron porphyrinates: Natural and synthetic hemes. *Inorg. Chem. 53*, 2582−2590.

(22) Phillips, G. N., Jr., Teodoro, M. L., Li, T., Smith, B., and Olson, J. S. (1999) Bound CO is a molecular probe of electrostatic potential in the distal pocket of myoglobin. *J. Phys. Chem. B 103*, 8817−8829.

(23) Andrew, C. R., Green, E. L., Lawson, D. M., and Eady, R. R. (2001) Resonance Raman studies of cytochrome *c′* support the binding of CO and NO to opposite sides of the heme: Implications for ligand discrimination in heme-based sensors. *Biochemistry 40*, 4115−4122.

(24) Andrew, C. R., Kemper, L. J., Busche, T. L., Tiwari, A. M., Kecskes, M. C., Stafford, J. M., Croft, L. C., Lu, S., Moënne-Loccoz, P., Huston, W., Moir, J. W. B., and Eady, R. R. (2005) Accessibility of the distal heme face, rather than Fe-His bond strength, determines the heme-nitrosyl coordination number of cytochromes *c′*: Evidence from spectroscopic studies. *Biochemistry 44*, 8664−8672.

(25) Chan, N.-L., Kavanaugh, J. S., Rogers, P. H., and Arnone, A. (2004) Crystallographic analysis of the interaction of nitric oxide with quaternary-T human hemoglobin. *Biochemistry 43*, 118−132.

(26) Xu, C., and Spiro, T. G. (2008) Ambidentate H-bonding by heme-bound NO: Structural and spectral effects of -O versus -N H-bonding. *J. Biol. Inorg. Chem. 13*, 613−621.

DOI: 10.1021/acs.biochem.5b00227
Biochemistry 2015, 54, 3320−3327

(27) Ibrahim, M., Derbyshire, E. R., Soldatova, A. V., Marletta, M. A., and Spiro, T. G. (2010) Soluble guanylate cyclase is activated differently by excess NO and by YC-1: Resonance Raman spectroscopic evidence. *Biochemistry 49*, 4864−4871.
(28) Hayashi, T., Miner, K. D., Yeung, N., Lin, Y. W., Lu, Y., and Moënne-Loccoz, P. (2011) Spectroscopic characterization of mono-nitrosyl complexes in heme-nonheme diiron centers within the myoglobin scaffold (Fe(B)Mbs): Relevance to denitrifying NO reductase. *Biochemistry 50*, 5939−5947.
(29) Lehnert, N., Sage, J. T., Silvernail, N., Scheidt, W. R., Alp, E. E., Sturhahn, W., and Zhao, J. (2010) Oriented single-crystal nuclear resonance vibrational spectroscopy of [Fe(TPP)(MI)(NO)]: Qualitative assessment of the *trans* effect of NO. *Inorg. Chem. 49*, 7197−7215.
(30) Tangen, E., Svadberg, A., and Ghosh, A. (2005) Toward modeling H-NOX domains: A DFT study of heme-NO complexes as hydrogen bond acceptors. *Inorg. Chem. 44*, 7802−7805.
(31) Xu, C., Ibrahim, M., and Spiro, T. G. (2008) DFT analysis of axial and equatorial effects on heme-CO vibrational modes: Applications to CooA and H-NOX heme sensor proteins. *Biochemistry 47*, 2379−2387.
(32) Dobbs, A. J., Anderson, B. F., Faber, H. R., and Baker, E. N. (1996) Three-dimensional structure of cytochrome *c′* from two *Alcaligenes* species and the implications for four-helix bundle structures. *Acta Crystallogr. D52*, 356−368.
(33) Kruglik, S. G., Lambry, J.-C., Cianetti, S., Martin, J.-L., Eady, R. R., Andrew, C. R., and Negrerie, M. (2007) Molecular basis for nitric oxide dynamics and affinity with *Alcaligenes xylosoxidans* cytochrome *c′*. *J. Biol. Chem. 282*, 5053−5062.
(34) Barbieri, S., Murphy, L. M., Sawers, R. G., Eady, R. R., and Hasnain, S. S. (2008) Modulation of NO binding to cytochrome *c′* by distal and proximal haem pocket residues. *J. Biol. Inorg. Chem. 13*, 531−540.
(35) Kekilli, D., Dworkowski, F. S. N., Pompidor, G., Fuchs, M. R., Andrew, C. R., Antonyuk, S., Strange, R. W., Eady, R. R., Hasnain, S. S., and Hough, M. A. (2014) Fingerprinting Redox and Ligand States in Haem Protein Crystal Structures using Resonance Raman Spectroscopy. *Acta Crystallogr. D70*, 1289−1296.
(36) Andrew, C. R., George, S. J., Lawson, D. M., and Eady, R. R. (2002) Six- to five-coordinate heme-nitrosyl conversion in cytochrome *c′* and its relevance to guanylate cyclase. *Biochemistry 41*, 2353−2360.
(37) Howes, B. D., Feis, A., Indiani, C., Marzocchi, M. P., and Smulevich, G. (2000) Formation of two types of low-spin heme in horeradish peroxidase isoenzyme A2 at low temperature. *J. Biol. Inorg. Chem. 5*, 227−235.
(38) George, S. J., Andrew, C. R., Lawson, D. M., Thorneley, R. N. F., and Eady, R. R. (2001) Stopped-flow infrared spectroscopy reveals a six-coordinate intermediate in the formation of the proximally bound five-coordinate NO adduct of cytochrome *c′*. *J. Am. Chem. Soc. 123*, 9683−9684.
(39) Russell, H. J., Harman, S. J., Heyes, D. J., Hough, M. A., Greetham, G. M., Towrie, M., Hay, S., and Scrutton, N. S. (2013) Modulation of ligand-heme reactivity by binding pocket residues demonstrated in cytochrome *c′* over the femtosecond-second temporal range. *FEBS J. 280*, 6070−6082.
(40) Huston, W. M., Andrew, C. R., Servid, A. E., McKay, A. L., Leech, A. P., Butler, C. S., and Moir, J. W. B. (2006) Heterologous overexpression and purification of cytochrome *c′* from *Rhodobacter capsulatus* and a mutant (K42E) in the dimerization region. Mutation does not alter oligomerization but impacts the heme iron spin state and nitric oxide binding properties. *Biochemistry 45*, 4388−4395.
(41) Tomita, T., Hirota, S., Ogura, T., Olson, J. S., and Kitagawa, T. (1999) Resonance Raman investigation of Fe-N-O structure of nitrosylheme in myoglobin and its mutants. *J. Phys. Chem. B 103*, 7044−7054.
(42) Thomas, M. R., and Boxer, S. G. (2001) ^{19}F NMR of trifluoroacetyl-labeled cysteine mutants of myoglobin: Structural probes of nitric oxide bound to the H93G cavity mutant. *Biochemistry 40*, 8588−8596.
(43) Vogel, K. M., Hu, S., Spiro, T. G., Dierks, E. A., Yu, A. E., and Burstyn, J. N. (1999) Variable forms of soluble guanylate cyclase: Protein-ligand interactions and the issue of activation by carbon monoxide. *J. Biol. Inorg. Chem. 4*, 804−813.
(44) Matsumura, H., Hayashi, T., Chakraborty, S., Lu, Y., and Moënne-Loccoz, P. (2014) The production of nitrous oxide by the heme/nonheme diiron center of engineered myoglobins (Fe(B)Mbs) proceeds through a trans-iron-nitrosyl dimer. *J. Am. Chem. Soc. 136*, 2420−2431.
(45) Reynolds, M. F., Parks, R. B., Burstyn, J. N., Shelver, D., Thorsteinsson, M. V., Kerby, R. L., Roberts, G. P., Vogel, K. M., and Spiro, T. G. (2000) Electronic absorption, EPR and resonance Raman spectroscopy of CooA, a CO-sensing transcription activator from *R. rubrum*, reveals a five-coordinate NO-heme. *Biochemistry 39*, 388−396.
(46) Tomita, T., Ogura, T., Tsuyama, S., Imai, Y., and Kitagawa, T. (1997) Effects of GTP on bound nitric oxide of soluble guanylate cyclase probed by resonance Raman spectroscopy. *Biochemistry 36*, 10155−10160.
(47) Lukat-Rodgers, G. S., and Rodgers, K. R. (1997) Characterization of ferrous FixL-nitric oxide adducts by resonance Raman spectroscopy. *Biochemistry 36*, 4178−4187.

DOI: 10.1021/acs.biochem.5b00227
Biochemistry 2015, 54, 3320−3327